



---

# Seismic damage avoidance design of moment resisting frames with innovative resilient connections

*S.M. Shabankareh, S. Veismoradi & P. Zarnani*

Auckland University of Technology, Auckland.

*P. Quenneville*

Auckland University, Auckland.

## **ABSTRACT**

Moment-resisting frames are one of the efficient lateral-load resisting systems in terms of providing architectural freedom in design and imposing smaller forces on foundations. Recent major earthquakes have resulted in significant plastic deformations in the beam-column connections causing irrecoverable damage in such structures. As a result, engineers have focused on developing new systems which not only provide the life-safety of the residents, but also minimise the damage such that the building could be reoccupied quickly after severe events with minimal business interruption and repair costs.

In this paper, a self-centring damage avoidance concept using the innovative Resilient Slip Friction Joint (RSFJ) is developed for steel Moment Resisting Frames (MRFs). The RSFJ provides the self-centring behaviour as well as energy dissipation in one compact component requiring no post-event maintenance. In this concept, the beam is connected to the column using a pin mechanism at the top, and the RSFJs at the bottom acting in tension and compression. The RSFJs allow for the gap opening in the connection during loading and re-centres the system upon unloading. Furthermore, a secondary collapse-prevention fuse is considered within the RSFJ to keep maintaining a ductile behaviour in the system in case of an event greater than the design earthquake.

In this paper, an analytical model is also developed to accurately predict the moment-rotation behaviour of this system. The seismic performance of the proposed concept is investigated by full-scale experimental testing. The test results validate the predictive model and demonstrate the efficiency of this new self-centring system for seismic damage avoidance design of MRFs.

## 1 INTRODUCTION

Seismic structural systems can be classified into different categories (Clifton et al. 2010). The first Category could refer to high damage structural designs or the conventional steel moment resisting frames.

In this category, fully restrained welded or bolted connections have been used between the beams and columns. Conventional moment frames are designed to dissipate energy under the design earthquake through yielding and formation of plastic hinges in the main structural members (Fig.1). As such, the structure gets damaged to prevent its collapse. The yielding in the plastic hinges can lead to significant inelastic deformations in the beams and columns, resulting in permanent structural damage as well as residual story drifts after the earthquake.

Most modern design codes are following the design philosophy of this first category, as they are based on an estimate of the demand and capacity. Since the plastic deformation generally happens, considerable repairs or replacements might be required after a major earthquake.

Usually, in this approach the design provides sufficient detailing to meet the desired performance objectives and plastic deformation is transferred to the pre-defined positions such as in the reduced beam sections.

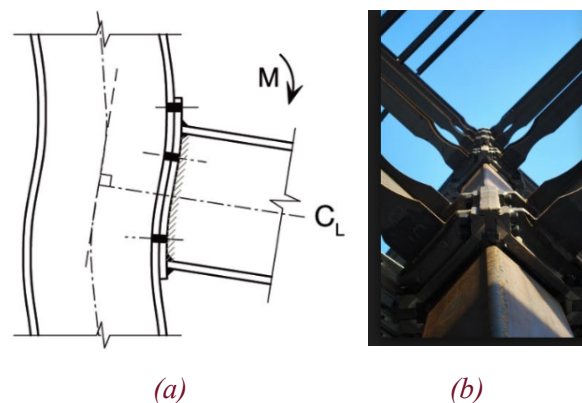


*Figure 1: High damage steel moment resisting frames a) Conventional MRF, b) Reduced beam section detailing for MRF*

The second category could refer to low-damage designs. One approach to accomplish this objective is to design the structure to be strong enough to prevent any inelastic/nonlinear behaviour, however this is generally uneconomical in terms of construction costs.

After the Northridge earthquake, several research projects were commenced to improve the conventional systems and introduce new concepts for steel frames to avoid inelastic deformations posed by the yielding of the structural elements (Roeder et al. 2000). The application of friction-based energy dissipating devices in steel structures dates back to 1982 when Pall et al. applied friction connections in braced frames to absorb the seismic energy. Clifton et al. (2007 and 2010) introduced the Sliding Hinge Joint (SHJ) as a low damage concept alternative to the traditional steel MRFs. The SHJ permits for gap opening in the beam-column contact area and energy dissipation by sliding movement of the plates.

To avoid structural damages and residual drift, post-tensioned beam-column connections for self-centring moment resisting frames (SC-MRFs) were proposed by Ricles et al. (2001). In which the gap opening in the contact zone of the beam-column connection gives the inelastic behaviour and the strands provide the self-centring. Later Garlock et al. (2002) proposed an empirical design procedure for steel PT frames based on the design earthquake loads.

This paper introduces a self-centring damage avoidance concept for steel MRFs using the innovative Resilient Slip Friction joint (RSFJ) technology (Zarnani and Quennville et al. 2015). The RSFJ provides self-

centring and energy dissipation through friction in one compact device requiring no post-event structural maintenance.

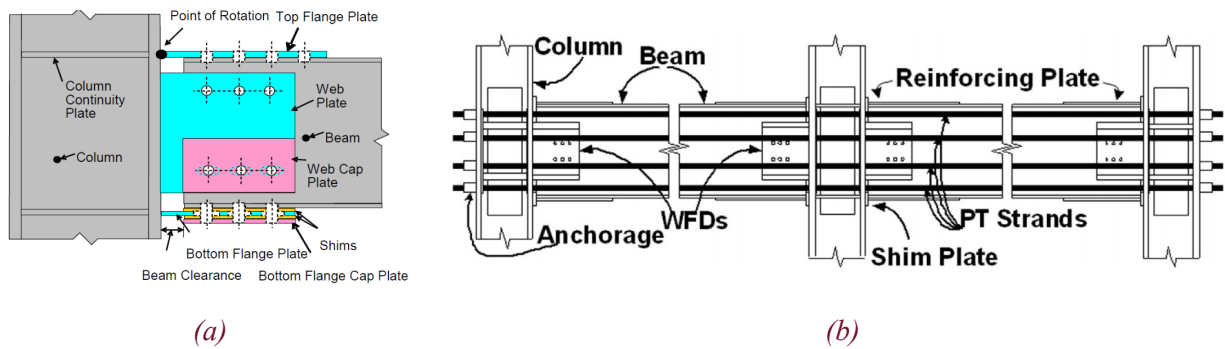


Figure 2: Category 2: a) Sliding Hinge Joint, b) PT self-centring MRF

## 2 RESILIENT SLIP FRICTION JOINT (RSFJ)

The concept of slip friction joints with the flat steel plates sliding over each other has always been recognized as an effective structural damping solution (Zarnani et al. 2015 and 2016). The energy dissipation mechanism of these joints is one of the most efficient amongst the passive damping technologies.

Nonetheless, the lack of self-centring behaviour in these joints potentially requires the use of another supplementary system, to re-centre the structure to its initial position which can be costly.

In this paper, a novel friction joint is presented in which the components are formed and arranged in a way that the self-centring behaviour is achieved as well as damping, all in one compact package. Figure 3 shows the components and the assembly for the RSFJ (Hashemi et al. 2016 and 2017). The specific shape of the ridges combined with the use of disc springs provide the required self-centring behaviour. The angle of the ridges is designed in a way that at the time of unloading, the reversing force induced by the elastically compacted disc springs is larger than the resisting frictional force between the sliding plates. Therefore, the elastic force of the discs re-centres the slotted sliding plates to their initial position.

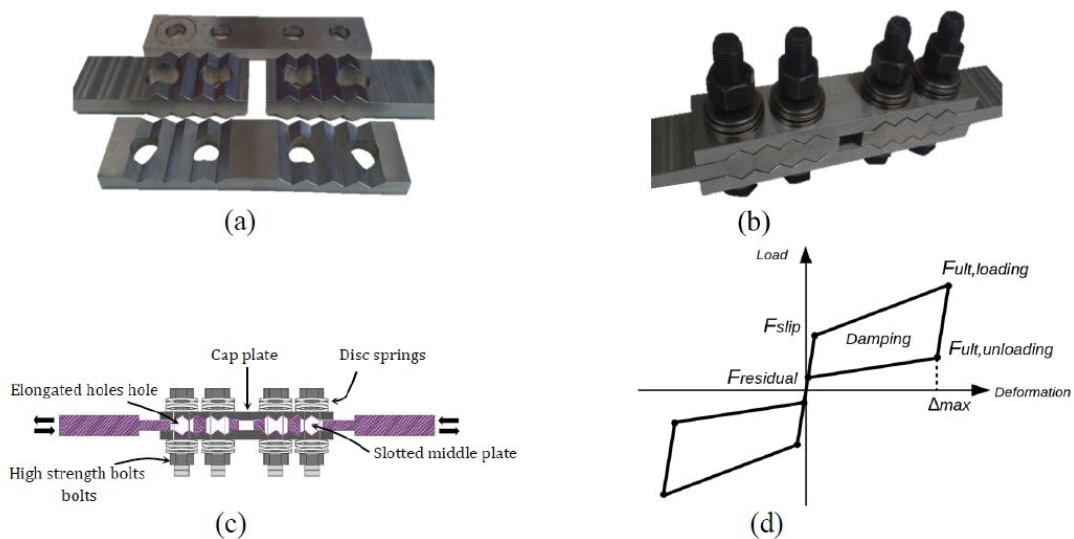


Figure 3: RSFJ: a) sliding plates, b) assembly, c) components, d) flag-shaped hysteresis

Figure 3 (d) displays the load-deformation behaviour of the RSFJ. The slip force ( $F_{slip}$ ) and the residual force ( $F_{residual}$ ) in the joint can respectively be determined by Eq.1 and Eq.2 where  $F_{b,pr}$  is the clamping force in the bolts,  $n_b$  is the number of bolts,  $\theta$  is the angle of the ridges,  $\mu_s$  is the static coefficient of friction and  $\mu_k$  is the kinetic coefficient of friction. The ultimate force in loading ( $F_{ult,loading}$ ) and unloading ( $F_{ult,unloading}$ ) can be calculated by replacing  $\mu_s$  and  $F_{b,pr}$  in Eq.1 and Eq.2 by  $\mu_k$  and  $F_{b,u}$ , respectively (Zarnani et al. 2016).

$$F_{slip} = 2n_b F_{b,pr} \left( \frac{\sin\theta + \mu_s \cos\theta}{\cos\theta - \mu_s \sin\theta} \right) \quad (1)$$

$$F_{residual} = 2n_b F_{b,pr} \left( \frac{\sin\theta - \mu_k \cos\theta}{\cos\theta + \mu_k \sin\theta} \right) \quad (2)$$

### 3 DAMAGE AVOIDANCE STEEL MOMENT RESISTING FRAMES (MRFs) USING RSFJ

The general concept of damage avoidance steel MRFs with RSFJs is demonstrated in Figure 4. In this new concept, the RSFJs are located along the bottom beam flange and consist of two middle plates and two cap plates. The two middle plates (with elongated holes) are attached to the beam bottom flange and the column. The two cap plates are clamped to the middle plates, and friction is generated when the middle plates slide against the cap plates. A pin is used at the top that can transfer the shear forces and axial loads. It should be noted since pure pin have almost zero construction tolerance, a shim plate may be used between the connection end plate and the column flange.

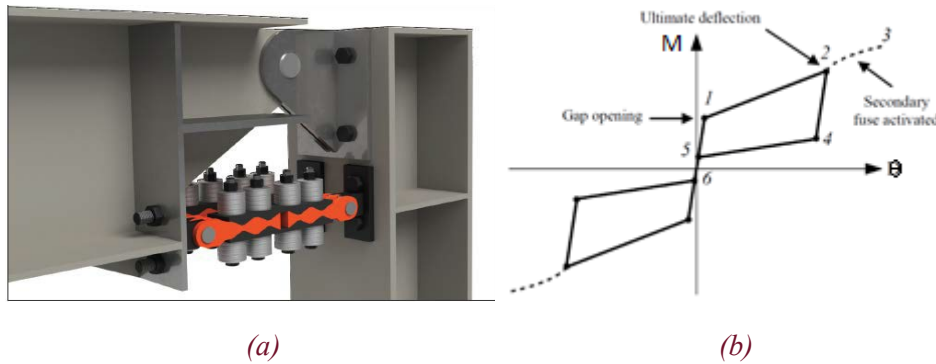
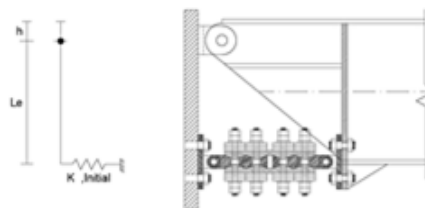


Figure 4: The concept of self-centring MRF with RSFJ: a) general arrangement, b) theoretical hysteresis

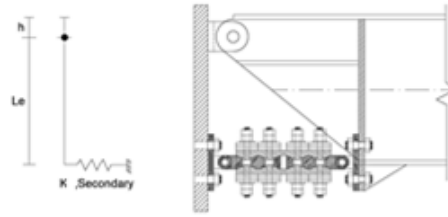
The conceptual relationship between the moment in the beam at the column face  $M$ , and the relative rotation between the beam and the column  $\theta_r$ , is shown in Figure 4 (b). Under the applied loading, the connection has an initial stiffness similar to that of a fully restrained bolted moment connection, where  $\theta_r$  is negligible (before slip at stage 1). In this phase, the total elastic stiffness of the RSFJs govern the stiffness of the connection. The beam connection is considered fixed and the stiffness of the entire system depends on beam and column stiffness. Once the applied moment overcomes the frictional resistance in the RSFJs, rotation and gap opening are imminent (at stage 1). Eq. 3 and Eq. 4 show the moment capacity of the connection at slipping point.



$$M_{slip} = F_{slip} \times L_e = (K_{initial} \times L_e \times \theta_{slip}) \times L_e = (K_{initial} \times L_e^2) \times \theta_{slip} = K_{\theta-initial} \times \theta_{slip} \quad (3)$$

$$K_{\theta-initial} = K_{initial} \times L_e^2 \quad (4)$$

After sliding, the moment capacity of the connection increases because the compaction of the disc springs produces additional axial force. The connection reaches the maximum capacity (stage 2) when the RSFJ reaches the ultimate capacity  $F_{RSFJ,ult}$ . Eq.5 and Eq. 6 show the ultimate moment capacity of the connection at the ultimate gap opening point.



$$M_{ult} = M_{slip} + M_{1-2} \quad (5)$$

$$\begin{aligned} M_{1-2} &= F_{ult-slip} \times L_e = (K_{secondary} \times L_e \times \theta_{ult-slip}) \times L_e = (K_{secondary} \times L_e^2) \times \theta_{ult-slip} \\ &= K_{\theta-secondary} \times \theta_{ult-slip} \end{aligned} \quad (6)$$

Note that if the load in the RSFJ continues to increase to more than  $F_{RSFJ,ult}$ , the secondary fuse can be activated (from stage 2 to stage 3). When the RSFJ reaches its maximum capacity and the ridges are locked, the clamping bolts (or rods) start to yield. The plastic elongation of the rods provides additional travel distance for the joint allowing it to maintain a ductile behaviour up to and even more than the collapse limit state of the structure. This means that when the RSFJ is designed for Ultimate Limit State (ULS) seismic loads (usually corresponds to 2.5% of inter-story drift), a ductile behaviour can be provided up to the Maximum Credible Earthquake (MCE), which is usually close to 4% of inter-story drift.

Upon unloading (from stage 2 to stage 4), the variation in  $\theta_r$  is insignificant. Between stages 2 and 4, moment contribution from the RSFJ changes direction due to a reversal of the friction force, where at stage 4 reversal of the friction force is complete. Between stages 4 and 5,  $\theta_r$  reduces as the beam comes back in contact with the column flange but is under compression. Between stages 5 and 6, the moment decreases to zero as the beam is fully compressed against the column face. A similar moment-rotation behaviour is expected in the opposite direction.

#### 4 COMPONENT TESTS OF THE RSFJ

In order to experimentally investigate the hysteretic behaviour of the RSFJ, a series of joint component tests were conducted. Fig. 5 displays the assembly of the manufactured specimen which comprised of two middle slotted plates and two cap plates. All plates were manufactured using mild steel grade 350. The angle of the grooves was 25 degrees. The testing has been conducted using a 210 kN axial load in Universal Test Machine with a load cell mounted on the crosshead above the RSFJ prototype to monitor the overall applied force.

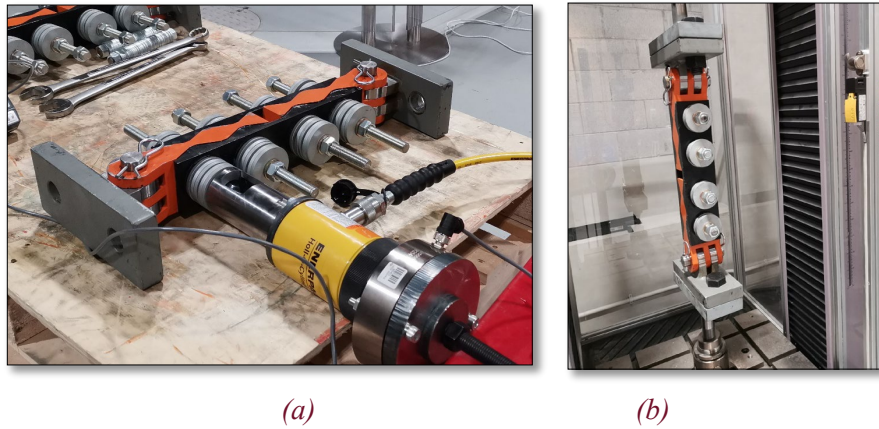


Figure 5: Component test: (a) Pre-stressing joint (b) Testing joint in UTM

Table 1 presents the design parameters and the capacity of the manufactured RSF joint based on the design procedure described in the previous sections. The slip force ( $F_{slip}$ ) was 150 kN.

Table 1: Characteristics of the tested RSFJ

Design Parameters	Value	Design Parameters	Value
Angle of the grooves	25	Disc spring thickness (mm)	6.5
Number of bolts (nb)	2	Disc spring overall height (mm)	8
$\mu$ s	0.10	Disc spring internal height (mm)	1.5
Slotted whole length (mm)	35	Disc spring outside diameter (mm)	70
Each washer capacity (kN)	130	Disc spring inside diameter (mm)	21
ns (Per bolt)	10		

From Figure 6, it can be seen that the load-deformation behaviour of the RSFJ represents “flag-shaped” hysteretic curves which imparts the self-centring behaviour as well as a significant rate of energy dissipation.

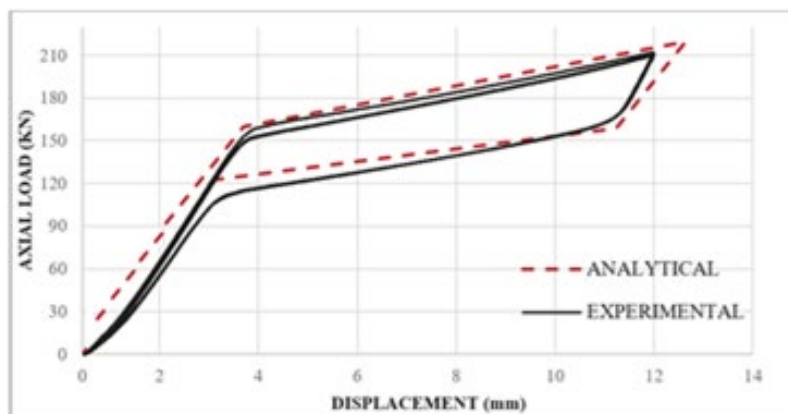


Figure 6: RSFJ component test results: Hysteretic behaviour

These results suggest that RSF technology has a high potential for the application in seismic resistant structures especially when a resilient damage avoidant design is required in order to protect the structures from major seismic events and the associated aftershocks.

## 5 NUMERICAL MODELLING OF THE STEEL MRFS WITH RSFJS

This section briefly describes the numerical modelling and analysis of steel MRFS with RSFJs.

The flag-shaped hysteresis of the RSFJ can be modelled using SAP2000 and ETABS providing the design parameters are properly calibrated. To study the behaviour of the RSFJs, a prototype joint is considered. Input data shows the specifications of the joint including the geometric properties, friction coefficient and specification of the disc springs. These analytical results showed that in the proposed model, flag shaped behaviour of the joint completely matched with experimental results.

Modelling in ETABS/SAP2000:

The RSFJ can be easily integrated in the structural analysis and design programs ETABS and SAP2000 (CSI 2011). It allows the designer to accurately calibrate the parameters according to the requirements of the project. In ETABS/SAP2000, the RSFJ can be modelled using the “Damper – Friction Spring” link Element. This function accurately represents the flag-shaped hysteresis of a RSFJ provided its parameters are properly calibrated in accordance with the design parameters of the joint. The parameters can be defined for any of the six translational or rotational degrees of freedom [16].

The design parameters of the RSFJ are,  $F_{slip}$  (slip force of the RSFJ),  $F_{ult}$  (ultimate force in the RSFJ at the end of loading),  $F_{restoring}$  (restoring force of the RSFJ),  $F_{residual}$  (residual force in the RSFJ at end of unloading),  $\Delta_{slip}$  (initial elastic deflection of the RSFJ before slip),  $\Delta_{ult}$  (ultimate displacement of the RSFJ),  $K_{initial}$  (initial stiffness of the RSFJ before slip),  $K_{loading}$  (loading stiffness of the RSFJ) and  $K_{unloading}$  (unloading stiffness of the RSFJ).

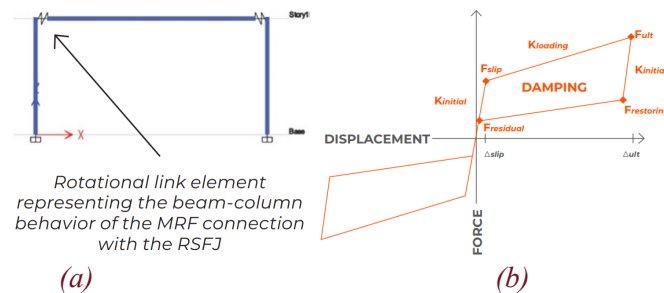


Figure 9: (a) SAP2000 modelling, (b) Design parameters

The recommended approach to model the MRFS with RSFJs is to model the moment-rotation behaviour of the beam-column connection using a single link element. The link element can be attached to the beam and column in their contact interface. The moment-rotation behaviour of the MRF connection can be specified respecting the force in the RSFJ ( $F_{RSFJ}$ ) and the lever arm ( $L_e$ ) which is the vertical distance between the centre of the RSFJ and the rotating pivot close to the top beam flange. For this case, the parameters should be defined for the related rotational degree of freedom (for example,  $R3$  when in the global “XZ” plane). The other five degrees of freedom should be “fixed”. The active direction should be defined as “Both” given the link element works in both directions.

Damper – Friction Spring design parameters:

- Initial (Non-slipping) Stiffness =  $K_{\theta-initial} = K_{initial} \times L_e^2$
- Slipping Stiffness (Loading) =  $K_{\theta-loading} = K_{secondary} \times L_e^2$
- Slipping Stiffness (Unloading) =  $K_{\theta-unloading} = K_{unloading} \times L_e^2$

- Pre-compression displacement =  $(-M_{slip}) / K_{\theta\text{-loading}} = - [(K_{\text{initial}} \times L_e^2) \times \Theta_{slip}] / [K_{\text{secondary}} \times L_e^2] = - (K_{\text{initial}} / K_{\text{secondary}}) \times \Theta_{slip}$
- Stop displacement =  $\Theta_{ult}$

By defining these parameters, the rest of the RSFJ parameters ( $\Theta_{slip}$ ,  $M_{ult}$ ,  $M_{restoring}$  and  $M_{residual}$ ) will be automatically adjusted.

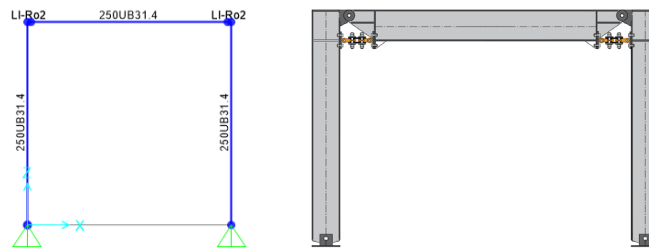


Figure 10: SAP2000 model and Position of RSFJ in MRF

To study the behaviour of the steel MRFs with RSFJs, a prototype frame is considered. Figure 10 (a) shows the specifications of the frame including the geometric properties and the frame sections. The frame has 4m, 3m width and height respectively and the columns are pinned to the foundation.

Table 2: Summary of the input data and design parameters for RSFJ

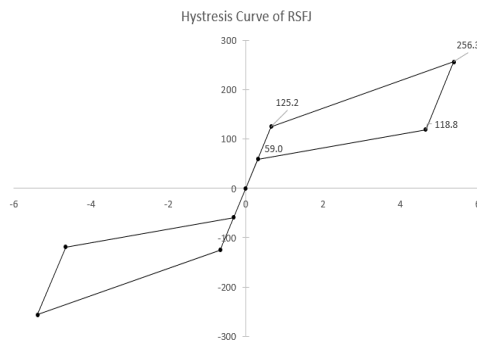
Input Parameter	Value	Design Parameter	Value
Angle of the grooves	35	Initial Stiffness (kN/mm)	7.6e6
$n_b$	1	Slipping Stiffness (Loading)	1.1e6
$\mu_s$	0.19	Slipping Stiffness (Unloading)	0.55e6
$F_{b,pr}$ (kN) = 50% $F_{b,ult}$	61	Pre-compression displacement	2.2%
Each washer capacity (kN)	135	Stop displacement (Rad)	2.5%
$n_s$ (Per bolt, each side)	2		

The required ULS moment capacities for the connections were determined as 50 kN.m. The slip threshold for the RSFJs is specified as 50% of the ULS moment capacity. Table 2 shows the input data and the calculated design parameters for the MRF connections.

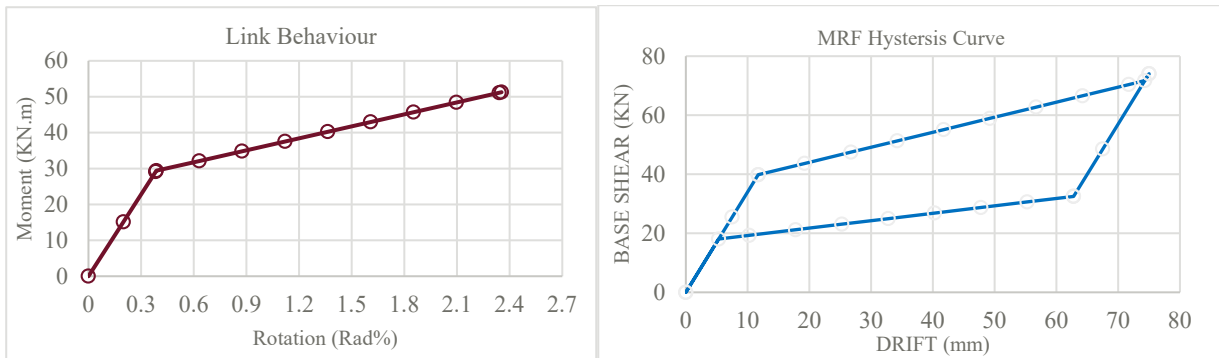
Push-over simulations were carried out for the frame with RSFJ. RSFJs were used for all of the connections.

Figure 11 (a) displays the moment-rotation curve for one of the connections. The Figure 11 (b) shows the base shear and the maximum story drift. It can be seen that the MRF connection shows a flag-shaped hysteresis with a fully re-centring behaviour.





(a)



(a)

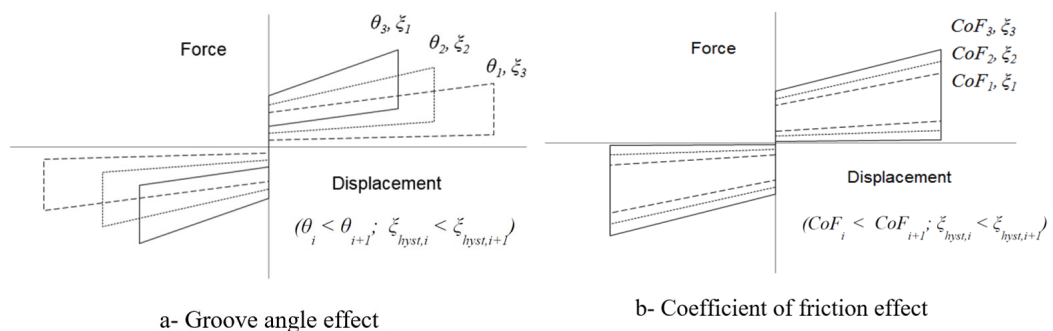
(c)

Figure 11: a) Theoretical hysteresis curve of RSFJ, b) Link behaviour, c) Hysteresis curve of MRF

## 6 CONNECTION PARAMETER EFFECTS

The cyclic hysteresis responses shown in Figure 12 illustrate the effect of connection parameters on its performance comprising of the variations in magnitude of the slip force, ultimate capacity, restoring force, residual resistance, joint displacement and hysteresis damping ratio ( $\xi_{hyst}$ ). The connection parameters studied consist of the angle of the groove, coefficient of friction (CoF), number of washers in series and parallel, number of the bolts, and the initial pre-stressing force of the bolts.

The difference between the  $F_{ult}$  and  $F_{restoring}$  indicates the frictional resistance that needs to be overcome during unloading to allow the joint to reverse back to its original position. As shown in Figure 12, by adopting a higher CoF (through different material arrangements for the sliding surfaces) and increasing the clamping force (through using more bolts), the frictional resistance increases accordingly, as theoretically expected. By comparing the connection parameters effect on the hysteresis damping ratio, it can be found that only the increment of the groove angle has a reverse effect on the  $\xi_{hyst}$ . Increasing the CoF, number of washers in parallel, and also the pre-stressing force result in a larger  $\xi_{hyst}$  while increasing the number of washers in series and number of bolts have no effect.



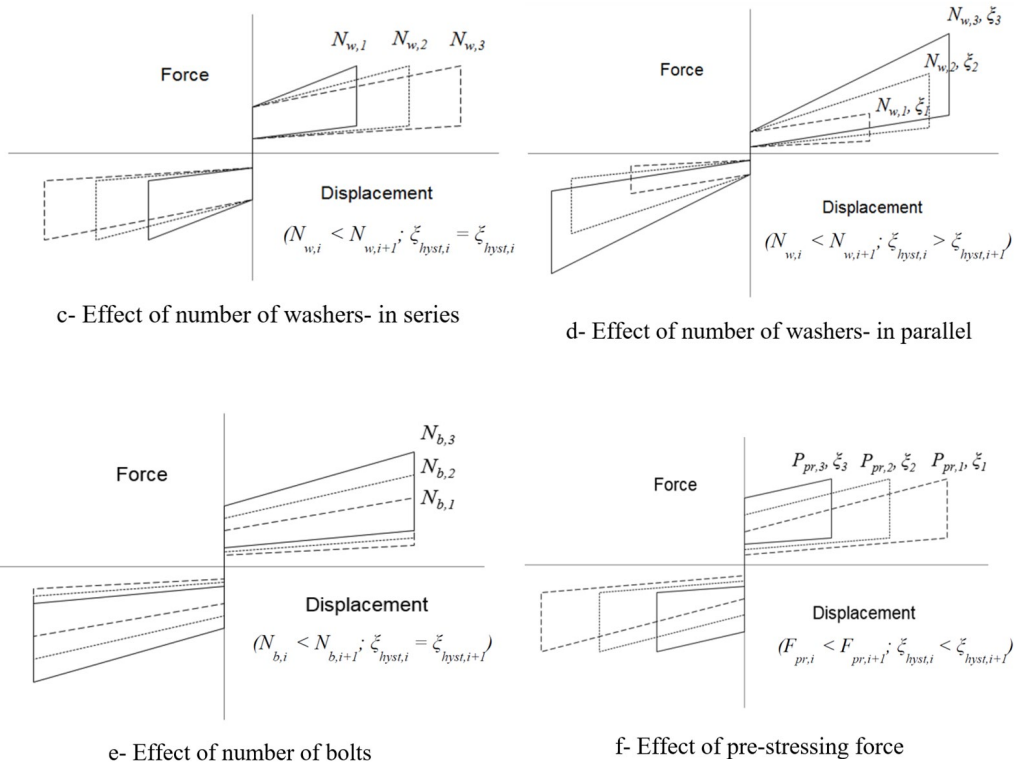
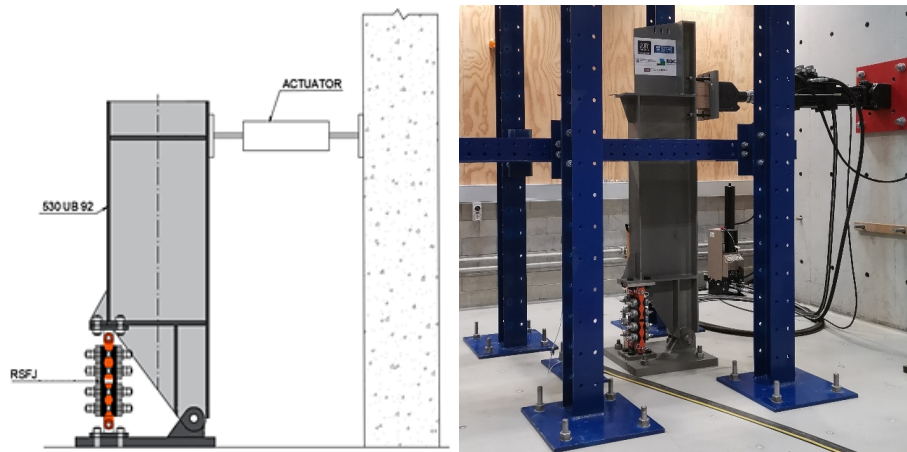


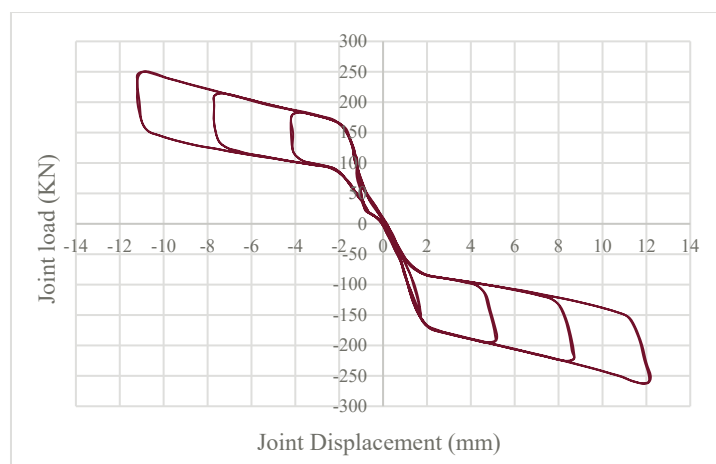
Figure 12: Effect of different parameters on connection performance

## 7 TEST SETUP

In order to verify the performance of the moment connection with RSFJ, a prototype test is planned (see Figure 13). The RSFJ has been designed for ultimate load of 350 kN (Figure 13(b)). The beam and connection have been designed based on NZS 3404 and ultimate moment equal to 300 kN.m. It should be noted that by increasing the number of bolts (in RSFJ) or length of lever arm (size of the beam), larger capacity could be achieved. In this test, RSF joint has totally four bolts and each bolt has three disc springs at each side. Angle of the grooves is 25 degree and pre-compressing force of discs is 80 kN. The connection will be tested for 250 kN.m moment.



(a)



(b)

Figure 13: a) MRF test setup with RSFJ, b) predicted hysteresis curve of RSFJ

## 8 CONCLUSIONS

This paper introduced the concept of damage avoidance self-centring steel Moment Resisting Frames (MRFs) using innovative Resilient Slip Friction Joints (RSFJs). In this concept, the RSFJ is connected to the bottom flange of the beam and the required ductility is provided by the gap opening in the beam-column contact surface. This connection offers a flag-shaped moment-rotation relationship demonstrating the self-centring behaviour. Furthermore, a secondary fuse within the RSFJ is introduced to prevent any brittle failure in the connection even when the applied force is higher than the design seismic load. In addition, experimental test result of moment steel connection with RSFJ demonstrated the seismic performance of the proposed system. Overall, the findings of this research confirmed an excellent seismic performance in terms of stability and self-centring behaviour.

## REFERENCES

Clifton G. C., MacRae G. A., Mackinven H., Pampanin S., and Butterworth J., "Sliding hinge joints and subassemblies for steel moment frames," in Palmerston North, New Zealand: Proc of New Zealand Society for Earthq Eng Conf, 2007.

- Clifton G. C., MacRae G. A., Mackinven H., Mago N., Butterworth J., and Pampanin S., "The sliding hinge joint moment connection," *Bull. New Zeal. Soc. Earthq. Eng.*, vol. 43, no. 3, p. 202, 2010.
- Computers and Structures, Inc, 2011. SAP2000: Structural Analysis Program, USA.
- Garlock M. Full-Scale testing, seismic analysis, and design of post-tensioned seismic resistant connections for steel frames [Ph.D. dissertation]. Bethlehem, PA: Dept. of Civil and Environmental Engineering, Lehigh University; 2002.
- Hashemi A., Masoudnia R., and Quenneville P., "A numerical study of coupled timber walls with slip friction damping devices," *Constr. Build. Mater.* vol. 121, pp. 373–385, 2016.
- Hashemi A., Masoudnia R., and Quenneville P., "Seismic performance of hybrid self-centring steel-timber rocking core walls with slip friction connections," *J. Constr. Steel Res.*, vol. 126, pp. 201–213, 2016. *Key Engineering Materials Vol. 763 733*
- Hashemi A., Zarnani P., Masoudnia R., and Quenneville P., "Experimental testing of rocking Cross Laminated Timber (CLT) walls with Resilient Slip Friction (RSF) joints," *J. Struct. Eng.*, vol. 144, no. 1, pp. 4017180-1-16, 2017.
- Pall A. S. and Marsh C., "Response of friction damped braced frames," *J. Struct. Eng.*, vol. 108, no. 9, pp. 1313–1323, 1982.
- Roeder C. W. and Venture S. A. C. J., *State of the art report on connection performance*. SAC Joint Venture, 2000.
- Ricles JM, Sause R, Garlock M, Zhao C. Post-tensioned seismic-resistant connections for steel frames. *J Struct Eng* 2001; 127(2):113–21.
- Zarnani, P. and Quenneville, P. (2015). "A resilient slip friction joint", Patent No. WO2016185432A1, NZ IP Office
- Zarnani, P., Valadbeigi, A. and Quenneville, P. (2016). "Resilient slip friction (RSF) joint: A novel connection system for seismic damage avoidance design of timber structures " *World Conf. on Timber Engineering WCTE2016*, Vienna Univ. of Technology, Vienna, Austria.